

A high resolution IC-calorimeter for the determination of heats of absorption onto thin coatings

D. Caspary, M. Schröpfer, J. Lerchner*, G. Wolf

Institute of Physical Chemistry, TU Bergakademie Freiberg, Leipziger Str. 29, D-09596 Freiberg, Germany

Received 18 May 1999; accepted 8 June 1999

Abstract

A miniaturized flow-through calorimeter based on silicon integrated thermopile chips has been developed. The flow-through calorimeter is applicable as sensor for the detection of volatile organic compounds as well as for the precise determination of heats of absorption of gases onto thin coatings. Applying fast and reversible reactions as it is the case for the absorption onto polymer coatings the resolution of the heat measurement is approximately 60 nJ. © 1999 Elsevier Science B.V. All rights reserved.

Keywords: Integrated circuit chip calorimeter; Heats of absorption; Coatings; Polymers

1. Introduction

The investigation of coatings of high sophisticated materials like supramolecular compounds, nano-sized particles and biologically relevant molecules and structures is of growing interest. Their widespread use as receptor materials for chemical sensors and chromatography promotes the development of new experimental techniques. For example, the monitoring of the gas absorption onto sensor coatings is possible now gravimetrically with a high degree of sensitivity applying quartz micro balances (QMB) [1]. A sufficient accurate prediction of the sensitivity and selectivity of gas sensor coatings requires a complete thermodynamic analysis of the absorption process. Therefore, practicable calorimetric measurement

techniques for the determination of heats of absorption onto sensor coatings are desirable. Recently different constructions and applications of integrated circuit (IC) calorimeters have been described [2]. In general the main part of an IC calorimeter consists of a silicon chip with integrated temperature transducer, calibration heater and heat sink. As an important advantage calorimeters with very low reaction volumes and time constants result in turn with the miniaturisation. We have already shown, that miniaturised flow-through calorimeters which are constructed on the basis of thermopile silicon chips can be applied as sensors for the gas detection [3]. With the presented paper a discussion of the optimal design of miniaturised flow-through calorimeters and their resolution and accuracy for the determination of heats of absorption onto thin coatings will be given. Because of the importance for gas sensors, application for the absorption of volatile organic compound onto polymer coatings will be demonstrated.

*Corresponding author. Tel.: +49-3731-39-2125; fax: +49-3731-39-3588
E-mail address: lerchner@erg.phych.tu-freiberg.de (J. Lerchner)

2. Experimental

2.1. Construction of the calorimeter

The calorimeter has been constructed on the basis of commercially available silicon chips LCM 2524 (Xensor Integration, Delft, NL) with integrated thermopiles (Fig. 1, [4]). The sensitivity for the heat power measurement is 2.4 V W^{-1} according to a thermal resistance of the silicon membrane of 34 K W^{-1} and a temperature coefficient of the thermopiles of 70 mV K^{-1} [2]. The thickness of the membrane ($30 \mu\text{m}$) is sufficient for repeatable coating procedures. The heat power is generated by absorption or desorption of the sample onto/from the polymer coated on the active area of the chip membrane. The heat conduction within the chip takes place with time constants of milliseconds. Even if relatively small samples are used the signal dynamics will not be determined by the transducer but mainly by the process dynamic. An electrically generated heat power step will be responded by an empty chip with an first order time constant of about 36 ms. The excellent dynamic behavior of the chip makes it possible to recognize heat transfer processes with time constants below 100 ms.

Two single thermopile chips are fixed within an aluminium frame and covered by a bottom plate and a stacked heat exchanger at the top (Fig. 2) to make up the calorimeter cell. A second chip can be applied for simultaneous reference measurements. The two reaction chambers where the gas flows contact the coating surface are enclosed by the etched hollows of the chips

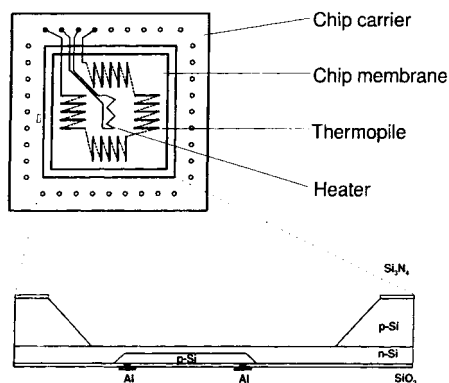


Fig. 1. Construction of the thermopile chip.

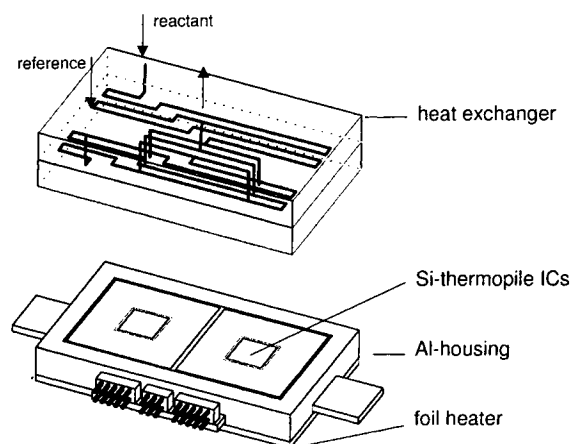


Fig. 2. Upper and lower part of the calorimetric cell. The upper part comprises the pipes for reactant and the heat exchanger consisting of aluminium plates with milled channels for the inlet gas flows. The lower part comprises an aluminium frame provided with two chip carriers and the bottom plate with an attached foil heater.

and the lower heat exchanger plate. An electrical foil heater for temperature control is attached at the bottom plate of the calorimeter. The supply of sample and reference gas (synthetic air) takes place via tube connectors in top of the calorimeter cell. The meandered channels milled into the heat exchanger plates serve for precise adaption of the temperature of the gas flows to that of the chip frames. Sample and reference gas flows are discharged into the calorimetric cell by alternate switching of two valves, as can be seen in Fig. 3. The sample gas will be generated using a thermostated vaporizer [5]. It is filled with an adsorbent (Chemosorb, Supleco, USA) containing the liquid sample. Leading inert gas through the vaporizer the gas flow will be saturated by the sample up to the equilibrium concentration according to the temperature of the vaporizer thermostat. To establish defined concentrations inert gas is added to the sample gas flow. The total flow as well as the concentration are determined by the settings of the three mass flow controllers (MFC). They are adjusted by a programmable scan controller. Control of the gas flow valves and the foil heater as well as data acquisition, data processing and information exchange with a communication device are performed by an electronic unit. The electronic unit, the calorimeter cell and the valves are housed in a compact module (Fig. 4). For

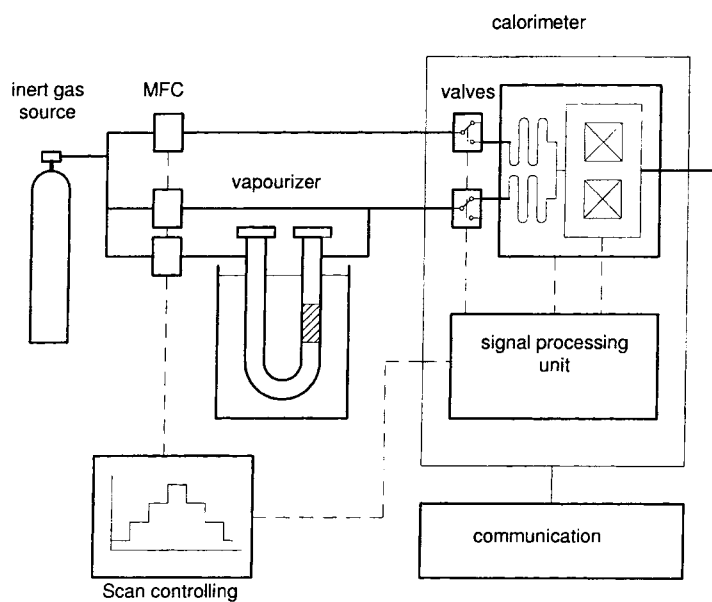


Fig. 3. Setup for calorimetric measurements. Reactant and reference are conducted into the measuring cell via two alternate switching valves.

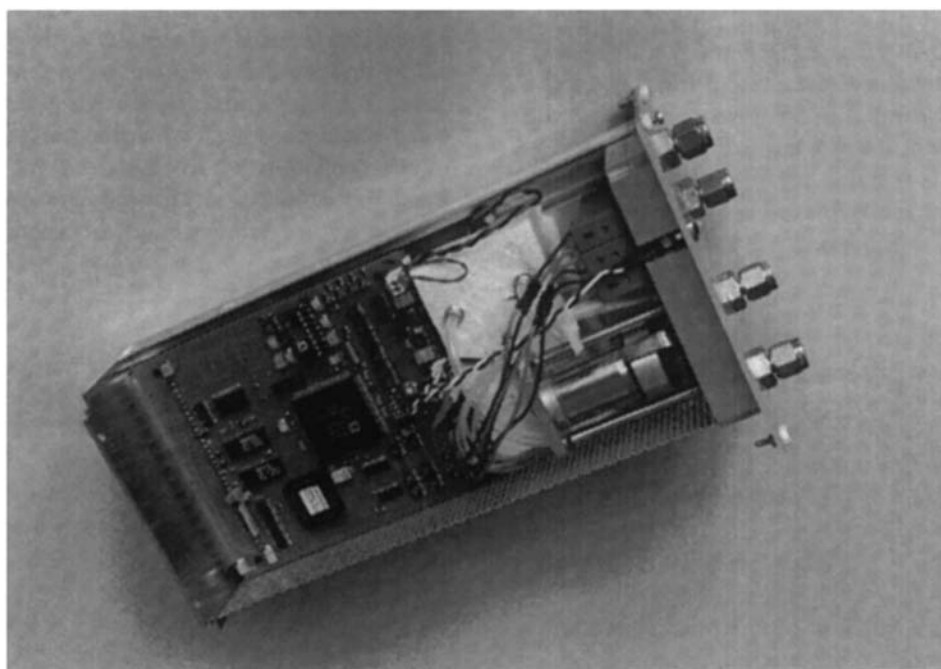


Fig. 4. Photograph of the calorimeter.

analytical applications which are not discussed here an internal pump can be used for gas flow control.

2.2. Preparation of the coatings

The coating of the thermopile chips has been performed by dropping of defined volumes of polymer solutions onto the surface of the chip membrane. After evaporation of the dichloromethane used as solvent the coated chips were heated up to 60°C for 2 h. For the calorimetric measurements the modified polysiloxanes polydimethylsiloxane (PDMS) and polyphenylmethylsiloxane (PPMS) (MoTech GmbH, Reutlingen) has been chosen. Because of the small active area of the chip membrane ($2 \times 2 \text{ mm}^2$) care has to be taken during the dropping of the polymer solution. The mass of the applied coatings was in the range 10–80 μg corresponding to a few μm .

3. Modelling

To optimize the design of the calorimeter and the operation conditions we have developed a model for the generation of the thermopile signal. Because a heat power signal refers to the change of the partial pressure of the sample, a maximum heat power signal requires a concentration step at the absorbing layer as rectangular as possible. The step will be flattened by the mixing behavior in the reaction chamber and by the absorption. Assuming uniform concentration in the reaction chamber the change of the sample concentration dc_{gas}/dt as response to an input concentration step c_0 ensues from the balance of the mass flows due to input and output gas flow and the rate of absorption of the sample molecules \dot{n}_{abs} according to

$$\frac{dc_{\text{gas}}}{dt} = \frac{\dot{V}(c_0 - c_{\text{gas}}) - \dot{n}_{\text{abs}}}{V_{\text{R}}} \quad (1)$$

with the flow rate \dot{V} and the volume of the reaction chamber V_{R} . The reduction of the sample concentration in the reaction chamber by absorption plays an important part if the diffusion of the sample molecules by the absorbent is faster than the delivery of the molecules by the gas flow.

The heat power is related to the rate of absorption

$$\dot{q}(t) = \Delta H_{\text{abs}}^0 \dot{n}_{\text{abs}} = \Delta H_{\text{abs}}^0 \frac{\rho_{\text{A}}}{m_{\text{A}}} \frac{dc_{\text{abs}}}{dt} \quad (2)$$

with the enthalpy of absorption ΔH_{abs}^0 and the mass m_{A} and the density ρ_{A} of the absorbent. In the equilibrium state the concentration of the sample within the absorbing coating c_{abs} is determined by the distribution coefficient K_{C} and the sample concentration in the reaction chamber c_{gas} :

$$c_{\text{abs}} = c_{\text{gas}} K_{\text{C}}. \quad (3)$$

The change of the sample concentration within the layer is controlled by diffusion, which can be calculated by Fick's law. In our model a state-space variable representation of the diffusion system is applied corresponding to the discretion of the coating into a limited number of layers with uniform sample concentrations. From the concentration gradient and the absorption enthalpy the heat dissipation in the absorbing layer as a function of time can be derived.

Regarding heat conduction within coating and membrane as well as heat loss due to heat exchange between surface and gas flow the temperature difference $\Delta T(t)$ across the thermopile can be described with the differential equation

$$C_{\text{Rez}} \frac{d\Delta T(t)}{dt} = \frac{1}{(R_{\text{Rez}}/R_{\text{TP}}) + 1} \dot{q}(t) - \left(\frac{1}{R_{\text{TP}} + R_{\text{Rez}}} + \frac{1}{R_{\text{Air}}} \right) \Delta T(t), \quad (4)$$

where C_{Rez} is the heat capacity of the absorbent, R_{Rez} the heat resistance of the absorbent, R_{TP} the heat resistance of the membrane with the thermopiles and, R_{Air} resistance for the heat transfer to the gas flow.

From the solution of the differential equation the thermovoltage $u(t)$ can be derived regarding the thermal sensitivity α_{S} of the thermopiles:

$$u(t) = \alpha_{\text{S}} \cdot \Delta T(t). \quad (5)$$

All numerical simulations and parameter optimizations were performed using the MATLAB-SIMULINK software system [6].

4. Results and discussion

4.1. Verification of the model

The model can be used to study the influence of design and operation parameters. For example, the

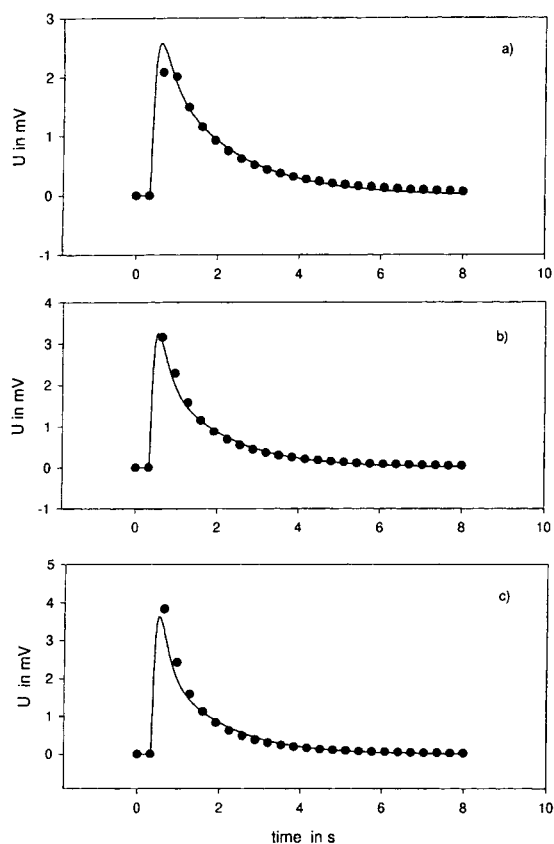


Fig. 5. Simultaneously performed fit to experimental data (4000 ppm ethanol, 40 μg PDMS) referring to different mass flows: (a) 40 ml/min, (b) 70 ml/min, (c) 100 ml/min.

signals for a concentration step of octane from 0 to 4000 ppm has been simulated and measured for three different flow rates (Fig. 5). As it is seen the flow rate influences the mixing time in the reaction chamber as well as the heat exchange between the absorbing layer and the gas flow. Unknown or not exactly known quantities as the diffusion coefficient of the absorbent, the active volume of the reaction chamber and the distribution coefficient for the absorption have been fitted to the three sets of measuring data simultaneously. There is a reasonable correspondence between the measured and the simulated data. Measurements with variable absorber masses also yield a good correspondence between the experimental and the simulated data. The remaining deviation is due to the idealisation of the geometry of the absorbing layer as well as the aerodynamics.

The model allows to investigate the influence of different design and operation parameters by simulation. The actual reaction chamber volume is about 65 μl . If it would be three times larger the dynamic would get worse (Fig. 6a). On the other hand a reduction of the volume by factor three yields a relative small dynamic profit. An increasing receptor mass (Fig. 6b) deteriorates the dynamic in a twofold manner: firstly by the deceleration of the diffusion, and secondly by the increasing absorption, whose contribution is shown in Fig. 6c. In Fig. 6d the influence of the dynamic properties of the coated silicon chip on the signal generation is demonstrated by performing simulations with and without consideration of the heat conduction inside the chip. The influence is clear, however it is not the essential contribution to the signal dynamics. This means that signal dynamics is essentially determined by the process dynamics.

4.2. Limit of heat detection

Fig. 7 depicts a thermopile voltage signal arising from a sequence of alternate absorption and desorption steps of ethanol (625 ppm) at PDMS. The base line shifts at the ends of the periods are due to the period wise mean value removal. The heats of absorption are determined from the peak areas using sensitivity data obtained from electrical calibration experiments. The absorption could be found reversible because peak heights and peak areas remain constant during a lot of absorption cycles. The mean values of the heat of absorption calculated from 50 cycles was found to be 1.12 μJ with a standard deviation of 0.45 μJ . The peak maximums correspond to a heat power of 2.6 μW . Analysis of the base line noise yielded 0.27 μW . Because the absorption is reversible, the signal-to-noise ratio can be increased by period wise accumulation of the signal. Fig. 8 depicts the dependence of the signal-to-noise ratio for the heat of absorption on the number of accumulation steps *nakku* which is not far from a square root dependence as expected for pure statistical noise. For an accumulation with *nakku* = 100 the signal shown in Fig. 9 results. The resolution could be improved to 62 nJ and 38 nW for heat and heat power detection, respectively.

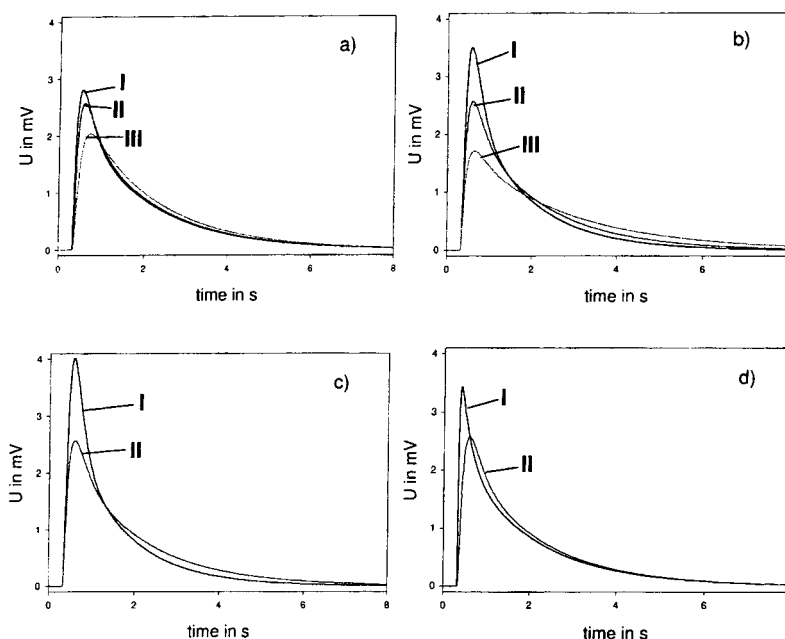


Fig. 6. Simulations of the signal varying some parameters: (a) the volume of the reaction chamber: I – 20 μl , II – 65 μl , III – 200 μl ; (b) the absorber mass: I – 10 μg , II – 40 μg , III – 100 μg ; (c) the influence of the step flattening by absorption: I – neglect the influence, II – regarding the influence; (d) the influence of the heat conduction: I – neglect the influence, II – regarding the influence.

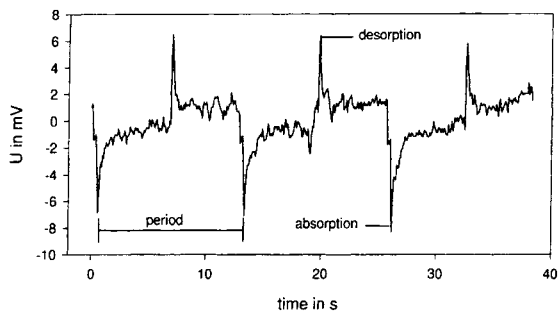


Fig. 7. Thermopile signal for a repeated absorption and desorption of 625 ppm ethanol at a very thin PDMS layer.

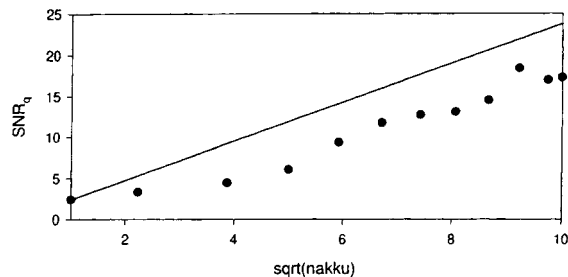


Fig. 8. Signal-to-noise ratio of the measured signal as a function of the square root of the accumulation number ($nakku$) and comparison to a square root dependency.

4.3. Estimation of the heat loss

Because of the lack of reliable test reactions for gas absorption [7], the estimation of the accuracy of the performed calorimetric measurements is restricted. The comparison with data from conventional calorimeters seems also to be questionable because of the need of larger sample masses and the different sample preparation. Main errors arise from the uncontrolled heat exchange between the surface of the coating and the gas flow. The heat loss due to forced convection

was estimated from the flow rate dependence of the signal parameters at constant heat power or heat pulses. Fig. 10 depicts the steady state signal voltage measured at constant electrical heat power of 0.1 mW and different flow rates including zero flow. Linearity can be observed for an empty as well as for a coated chip. This allows us to conclude that the flow conditions and hence the nature of the heat exchange between surface and gas flow do not differ markedly in both cases. Therefore, a linear extrapolation to zero flow should be possible also in the case of absorption

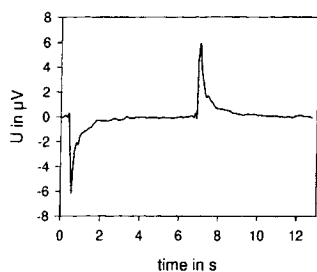


Fig. 9. Average of 100 periods of the thermopile signal referring to Fig. 7.

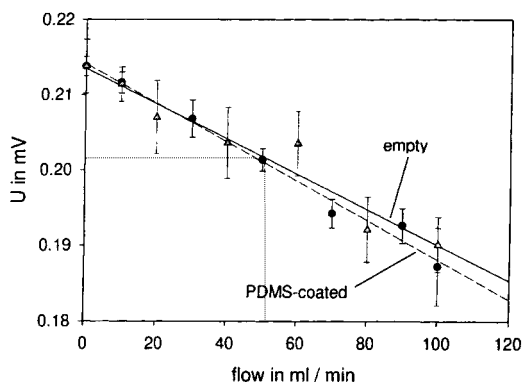


Fig. 10. Steady state signal voltage versus flow due to electrical heating for an empty (a) and a PDMS coated (b) chip.

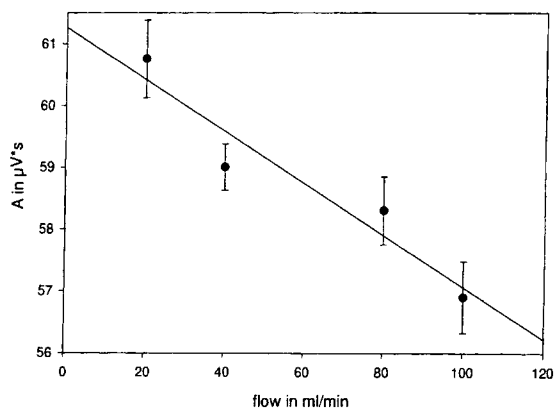


Fig. 11. Peak area as function of flow for the absorption of 4600 ppm ethanol for the absorption of ethanol at PDMS.

measurements. Assuming this, from Fig. 11 can be seen, that the heat loss at a typical flow rate of 100 ml min^{-1} corresponds to an error of approxi-

mately 8%. The error can be reduced by extrapolation to zero flow to 0.5%. The heat loss should be nearly independent for different samples. Therefore, the heat loss determination is necessary only once for every coating.

4.4. Precision of the coating procedure

The heat values have to be referred to the mass of the coated layer. Therefore, a coating as precise as possible is necessary. To determine the precision of the coating measurements with repetitive coated chips has been performed at equal conditions. As a result the detected heats of absorption varied with a relative standard deviation of 4% for a layer of $40 \mu\text{g}$. Because the scatter of the measured heats for a given coating is much lower ($<1\%$) this variations are probably due to deviations of the mass of the coating. The application of micromechanical pipettes for the drop coating should be overcome this limitations in the future. Fig. 12 depicts the dependence of the peak area on the mass of the coating. The deviations from the straight line are due to mass variations too.

5. Conclusions

One of the outstanding properties of integrated circuit chip calorimeters are their low time constants.

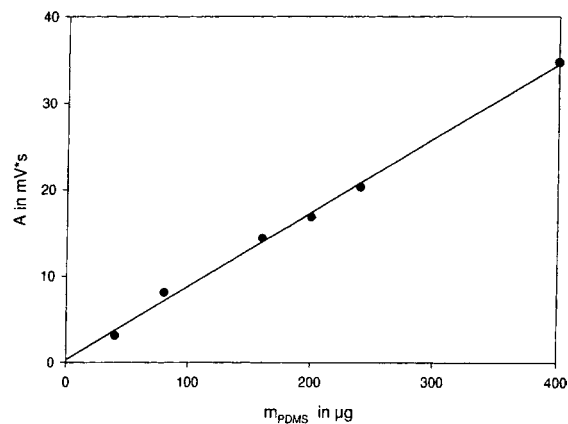


Fig. 12. Peak area for the absorption of 2000 ppm octane at PPMS versus the mass of the layer.

As a consequence short heat power pulses with a pulse width of only a few seconds are detectable without markedly attenuation. In such a case the limit of detection for the heat measurement becomes some orders lower in comparison with conventional heat flow calorimeters even if the static sensitivity and heat power resolution are similar. Therefore, the developed calorimeter should be a powerful tool for calorimetric investigations at thin coatings. For example, first experiments have shown that the discrimination of gaseous enantiomers absorbed by optically active coatings, i.e. modified cyclodextrines, can be examined calorimetrically.

References

- [1] K. Bodenhöfer, A. Hierlemann, G. Noetzel, U. Weimar, W. Göpel, *Anal. Chem.* 68 (1996) 2210.
- [2] J. Lerchner, A. Wolf, G. Wolf, *J. Thermal Anal.* 57 (1999) 241.
- [3] J. Lerchner, D. Caspary, G. Wolf, M. Krügel, M. Nietzsche, *Proc. Sensor 97 Nürnberg*, 1997.
- [4] A.W. Van Heerwarden, P.M. Sarro, *Sensors and Actuators* 10 (1986) 321.
- [5] K. Bodenhöfer, A. Hierlemann, R. Schlunk, W. Göpel, *Sensors and Actuators B* 45 (1997) 259.
- [6] Math Works, Natick, USA.
- [7] I. Wadsö, 14. Ulm-Freiburger Kalorimetrietage, Freiberg, 1999.